E-ISSN 2586-9027
Homepage : https://tci-thaijo.org/index.php/SciTechAsia Science & Technology Asia
Vol.31 No.3 July - September 2026 Page: [187-197]
Original research article

Computation of SAR and Temperature Increase in Human Eye Exposed to 5G Radiation

Deepshikha Bhargava[1,*], Nannam Sriploy[1], Napat Suradinkura[1], Vasit Sirilapanan[1], Phadungsak Rattanadecho[2]

[1]*Department of Mechanical Engineering, Faculty of Engineering, Kasetsart University, Bangkok 10900, Thailand*
[2]*Center of Excellence in Electromagnetic Energy Utilization in Engineering, Department of Mechanical Engineering, Faculty of Engineering, Thammasat University, Pathum Thani 12120, Thailand*

Received 13 April 2026; Received in revised form 5 August 2026
Accepted 10 August 2026; Available online 30 September 2026

ABSTRACT

The rapid deployment of fifth-generation (5G) wireless communication systems has raised questions regarding the potential biological impacts of prolonged exposure to radiofrequency electromagnetic (RF-EM) radiation. Due to the sensitivity of ocular tissues, this study investigates the interaction between 5G electromagnetic waves and the human eye. A two-dimensional computational model of the human eye was developed and subjected to EM exposure at various 5G operating frequencies. The resulting electric field distribution, specific absorption rate (SAR), and temperature increase caused by RF energy absorption were evaluated. A coupled multiphysics approach was implemented using Maxwell's equations to simulate EM wave propagation through the eye tissues and the Pennes bioheat transfer equation to estimate temperature variations within different ocular layers. The coupled EM–thermal analysis was performed using the finite element method (FEM). The results indicate that, under certain exposure conditions, the resultant SAR and temperature values exceeded the threshold values.

Keywords: 5G radiation; Human eye; Finite element method; Specific absorption rate; Temperature increase

***Corresponding author:** deepshikha.b@ku.th doi.org/10.70730/sta.v31i3.268408

1. Introduction

The ongoing debate surrounding the potential harmful effects of microwave radiation exposure has sparked significant interest. Microwave radiation, a type of non-ionizing radiation operating within the 300 MHz to 300 GHz frequency range, is prevalent in our daily lives through various devices, including cell phones, wireless routers, and microwave ovens. While generally considered safe due to its non-ionizing nature, concerns about its impact on health have arisen, with reports of headaches, nausea, and confusion among those frequently exposed [1, 2]. To address these concerns, organizations like ICNIRP and IEEE have established guidelines to limit human exposure to EM radiation. These guidelines use Specific Absorption Rate (SAR) as a measure, which tells us the absorbed electromagnetic (EM) radiation in the tissues per unit mass. The ICNIRP has set a threshold SAR value of 2 W/kg for 10-gram tissues. Furthermore, excessive thermal elevation in ocular tissues may lead to adverse effects, where an increase of approximately 3–4 °C has been associated with cataract development, while temperatures reaching around 41 °C may contribute to posterior capsular opacities (PCO) formation [3, 4].

With the advent of high-speed 5G radiation, there are new installations of high-powered radio stations and new devices entering the market. 5G radiation comes under the non-ionizing spectrum of EM radiation, as shown in Fig. 1. Though it is non-ionizing and very low in comparison to the ionizing radiations such as x-rays, and gamma rays, the frequency used for the 5G radiation is very high [2]. The human eye is considered a highly sensitive organ due to its complex structure and limited external protection. Among all 5G radiation-emitting devices, mobile phones are likely the most commonly used by humans today. Therefore, evaluating the possible effects of 5G radiation absorption in eye tissues is important for understanding potential exposure-related thermal and biological responses.

Awada et al [5], investigated the possible biological implications of exposure to 5G electromagnetic fields; using a Specific Anthropomorphic Mannequin (SAM) phantom and CST software, they simulated the SAR on the human brain due to 5G exposure for two frequency candidates (29 and 33GHz). Their findings indicated that the SAR for both candidates exceeded the safety exposure limit, suggesting potential health concerns. However, the study emphasized the need for further research to determine the SAR values for more individuals and to study the impact of 5G waves on the human head under various conditions.

Kaburcuk, F. et. al [6] investigated the influence of 5G electromagnetic exposure on the absorption characteristics and thermal response of the human head. Using a Multiphysics model, they analyzed the SAR and temperature rise distributions in the head, considering factors such as frequency and incident angle. The study concluded that both SAR and temperature rise were dependent on the frequency and incident angle, with the maximum values occurring in the eyes. The Multiphysics model also proved to be computationally efficient for analyzing multiple frequencies. However, the research does not include electric field distribution.

Aru et. al. [7] utilized machine learning techniques to study the potential health risks of 5G radiation exposure. They used artificial neural networks to model the absorption and penetration of 5G EM energy into human DNA. Their results suggested

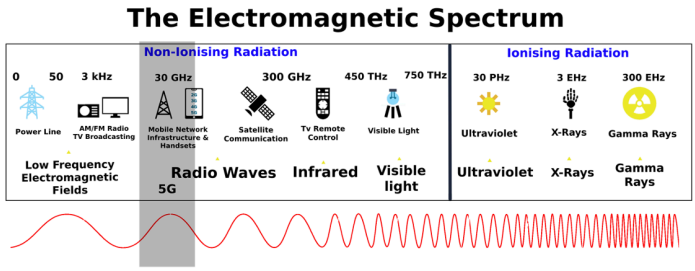


Fig. 1. Electromagnetic spectrum.

that the non-ionizing radiation emitted by 5G technology is not powerful enough to break DNA chemical bonds or cause cellular changes leading to cancer or viral diseases. However, the study does not focus on the absorption of the radiation in the human eye. Aricioglu et. al [8], studied the effect of 5G radiation on human eye tissues. They calculated the electric field and temperature distribution in a 2D eye model using the Transmission Line Model (TLM) and the Finite Element Method (FEM). The temperature in the eye exceeded the threshold value for cataract formation at a 3.8 GHz frequency.

While previous studies have provided valuable insights into the effects of 5G EM radiation on the human eye, several aspects remain insufficiently explored. Many existing studies have evaluated the electric field, specific absorption rate (SAR), and thermal response under selected exposure conditions, typically considering a limited number of operating frequencies or fixed radiated power levels. In contrast, the present study systematically investigates the combined effects of multiple 5G frequency bands and radiated powers on the electric field distribution, SAR, and temperature increase in a realistic heterogeneous 2D human eye model. This comprehensive assessment provides a clearer understanding of how both frequency and radiated power influence EM energy absorption and the resulting thermal response in ocular tissues.

2. Physical Model

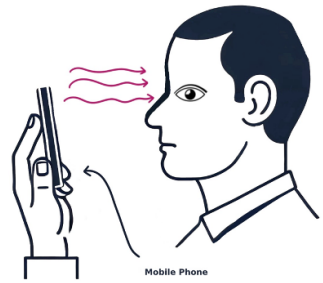


Fig. 2. Human eyes getting exposed to the 5G radiation from a cell phone.

The 5G radiation source irradiates the eye model from the left side, as shown in Fig. 2, with the help of a port boundary condition. The distribution of electric field intensity, Specific Absorption Rate (SAR), and temperature variation within the individual layers of the eye was evaluated using a coupled EM and thermal analysis based on the finite element method (FEM). The dielectric and thermal parameters assigned to the eye tissues are provided in Table 1 [5, 9] and Table 2 [10], respectively. The objective of this work is to analyze the interaction between 5G EM exposure and different anatomical regions of the human eye. A 2D human eye model is modelled consist-

ing of – cornea, lens, anterior chamber, iris, posterior chamber, vitreous, and sclera, as shown in Fig. 3 [8]. Although the adopted 2D model captures the essential trends of electromagnetic energy absorption and heat transfer in the eye, it cannot fully represent the complex three-dimensional (3D) geometry of the human eye or the inherently three-dimensional exposure produced by a mobile phone. Therefore, the results should be interpreted as simplified numerical investigation, and future work will extend the present analysis to a realistic 3D computational model.

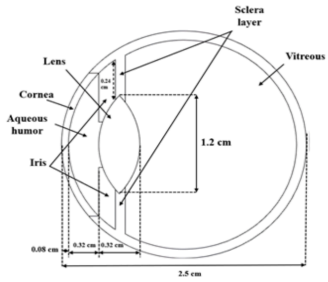


Fig. 3. Heterogenous model of human eye.

Five 5G operating frequencies (2.6, 3.6, 4.4, 18, and 30 GHz) are considered in this study. The eye is exposed to these frequencies at a radiated power of 0.1 W for the frequency comparison, while additional simulations are performed at radiated powers of 0.05 W, 0.1 W, and 1 W to investigate the influence of input power on SAR and temperature rise. The EM field distribution was obtained by solving Maxwell's equations, whereas the corresponding thermal response was evaluated using the Pennes bioheat transfer Eqs. (3.4)-(3.5).

3. Mathematical Model

3.1 Electromagnetic wave propagation model

The propagation of electromagnetic waves through the ocular tissues and the surrounding medium was analyzed numerically by applying Maxwell's equations. A 2D computational approach was adopted to decrease the simulation complexity and computational cost while maintaining sufficient accuracy of the obtained results. For the EM analysis, the following assumptions were considered:

(1) The interaction between the incident EM wave and the eye tissues is represented using a 2D model.

(2) The computational domain surrounding the eye structure is terminated using a scattering boundary condition to minimize reflections.

(3) The dielectric characteristics of the eye tissues are assumed to be homogeneous and remain unchanged during the simulation.

(4) The EM excitation is considered to operate in the Transverse Electric (TE) mode [4]

$$\nabla \times \left(\frac{1}{\mu_r \nabla \times E} \right) - k_0^2 \left(\varepsilon_r - \frac{j\sigma}{\omega \varepsilon_0} \right) = 0, \tag{3.1}$$

where E refers to Electric field (V/m), μ_r is relative magnetic permeability, ε_r is the relative dielectric constant, $\varepsilon_0 = 8.8542 \times 1012$ F/m is permittivity of free space, σ denotes electrical conductivity (S/m), and k_0 refers to free space wave number $(m1)$.

The area outside the eye model is truncated using the scattering boundary condition [4], Eq. (3.2).

$$n(\nabla \times \vec{E}) - jkn \times (\vec{E} \times n)$$
$$n \times (\vec{E}_0 \times jk(n-k)\exp(-jk \cdot r)), \tag{3.2}$$

Table 1. Dielectric Properties of the eye at different 5G frequencies [5, 9].

Tissues	2.6 GHz		3.6 GHz		4.4 GHz		18 GHz		30 GHz	
	ε_r	σ(S/m)	ε_r	σ(S/m)	ε_r	σ(S/m)	ε_r	σ(S/m)	ε_r	σ(S/m)
Cornea	51.4	2.4	49.8	3.26	48.6	4.01	30.3	22.2	20.9	34.2
Lens	33.8	1.16	32.8	1.76	32	2.32	19.1	14.2	13	21.4
Vitreous	68.1	2.6	67.3	3.58	66.5	4.56	42.9	33.4	26.7	53.2
Iris	52.5	1.84	51.3	2.65	50.3	3.41	33	22.1	23.2	35.5
Aqueous humor	66.6	3.6	64.4	4.69	63	5.73	39.2	29.9	26.6	46
Sclera	52.4	2.15	51	3.01	49.9	3.83	31.2	22.5	21.5	35

Table 2. Thermal properties of the eye [10].

Tissue	ρ(kg/m^3)	k(W/°C)	C_p(J/kg°)
Cornea	1050	0.58	4178
Lens	1000	0.4	3000
Vitreous	1100	0.603	4178
Iris	1050	1.0042	3180
Aqueous humor	996	0.58	3997
Sclera Layers	1050	1.0042	3180

where k is the wave number ($m1$), σ is the electric conductivity (S/m), n is normal vector, $j = \sqrt{1}$, and E_0 is the incident plane wave (V/m).

The incident EM wave travels through the surrounding medium before interacting with the eye, where a portion of the EM energy is absorbed by the eye. This absorbed power deposition is quantified using SAR, which represents the rate of EM energy absorbed per unit mass of tissue: [6].

$$SAR = \frac{\sigma}{\rho}|E|^2. \tag{3.3}$$

3.2 Bioheat transfer model

For calculating the temperature distribution, thermal properties of the eyes from Ooi E-H et. al [10] are used, shown in Table 2.

The temperature variation within the eye tissues was determined by applying the classical heat transfer equation. The initial temperature of the eye model was considered to be 37 °C. To simplify the thermal simulation and reduce computational complexity, the following assumptions were applied:

1. The thermal characteristics of the eye tissues are considered homogeneous and constant throughout the analysis.
2. The biological tissues are treated as thermally active biomaterials.
3. No additional effects such as internal energy generation, phase transformation, or chemical reactions are considered during the simulation.

The transient heat conduction formulation was employed to estimate the temperature distribution inside the eye tissues. This approach provides an effective method for evaluating heat transfer mechanisms within biological materials [11], Eq. (3.4)

$$\rho C\frac{\partial T}{\partial t} = \nabla\cdot(k\nabla T) + \rho_b C_b \omega_b (T_b - T) + Q_{met} + Q_{ext}, \tag{3.4}$$

where ρ refers to tissue density (kg/m^3), C_p is the heat capacity of tissue (J/kg °C), k is the thermal conductivity of tissue (W/m °C), T is the tissue temperature (°C), and Q_{ext} is the external heat source term (EM heat-source density) (W/m^3), defined as [11]:

$$Q_{ext} = \frac{1}{2}\sigma_{tissue}|E|^2 = \frac{\rho}{2}\cdot SAR. \tag{3.5}$$

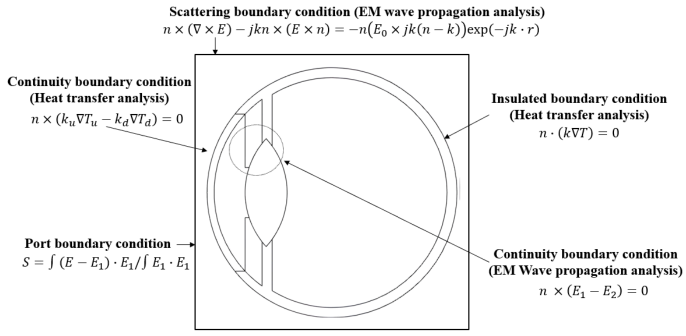


Fig. 4. Boundary conditions for Electromagnetic wave and Bioheat Transfer.

A thermal insulation boundary condition was imposed on the external boundary of the eye model to prevent heat exchange with the surrounding environment [11]:

$$n \cdot (k \nabla T) = 0. \tag{3.6}$$

A continuous thermal interface is assumed between adjacent ocular layers, indicating that heat transfer occurs directly across the tissue boundaries without any additional contact resistance [11].

$$\nabla T_u = \nabla T_d, \tag{3.7}$$

$$n \cdot (k_u \nabla T_u - k_d \nabla T_d) = 0 \tag{3.8}$$

The finite element method (FEM) was employed to solve the coupled EM and transient thermal problems in the 2D human eye model. First, Maxwell's equations were solved to determine the electric field distribution and the corresponding EM power absorption within the ocular tissues. The calculated absorbed power was subsequently used as the heat source in the Penne's bioheat transfer equation to predict the transient temperature distribution. A refined mesh was employed in regions of interest to ensure numerical accuracy. The coupled EM–thermal simulations were performed using COMSOL Multiphysics. The transient thermal analysis was carried out over an exposure duration of 30 min using the COMSOL time-dependent solver with automatic time stepping. The temperature distributions presented in this study correspond to the final simulation time at the end of the 30 min exposure period.

4. Results and Discussions

4.1 Validation with literature

from the literature is followed step by step. A 2D eye model, same as in the study of Aricioglu et. al [8], is exposed to an EM source radiating at 700MHz frequency, and 0.35mW radiated power. The temperature distribution obtained from the current simulation was compared with the reported results, as presented in Fig. 5. As can be seen, the present study shows good results when compared with literature. This indicates that the method and model in the proposed study are reliable. Additionally, a mesh independence analysis was conducted to evaluate the influence of mesh density on the simulation outcomes. Fig. 6 illustrates the generated 2D mesh of the eye model along with the variation of temperature results corresponding to different mesh element counts. After 4562 mesh elements, the temperature becomes independent and shows steady results.

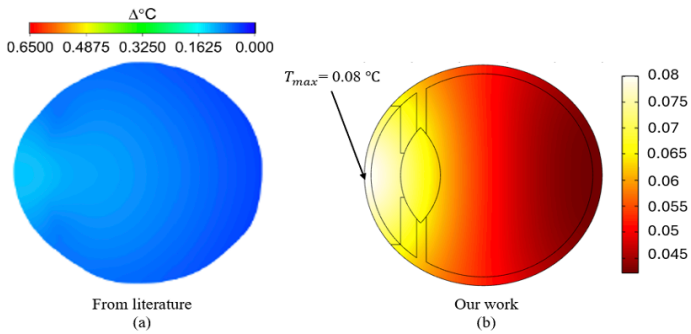


Fig. 5. Temperature distribution in the eye for 700 MHz frequency at 0.35 mW power (a) literature, and (b) present work.

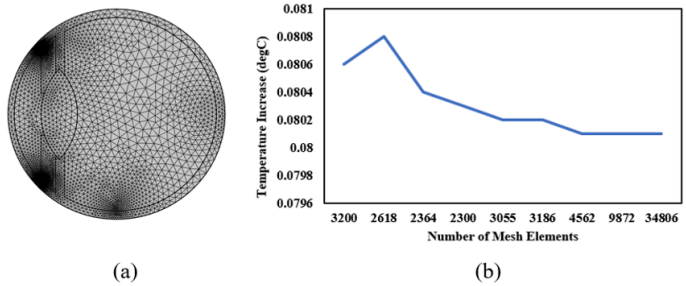


Fig. 6. (a) 2D mesh model of human eye, and (b) mesh convergence graph between temperature and mesh elements.

4.2 Electric field distribution

EM radiation in TE mode propagates from the left side and is incident on the eye (Fig. 4). The propagation of these EM waves in the outer space of the eye and inside the eye tissue is obtained by solving Maxwell's equation, Eq. (3.1). Upon interaction with the eye tissues, part of the radiation is absorbed, while some is reflected and refracted. Fig. 7 illustrates the electric field distribution in the eye tissues at various 5G frequencies. The results indicate that the electric field is primarily concentrated in the outer layers - cornea, aqueous humor, and lens. The observed electric field distribution is governed by the dielectric properties of the ocular tissues (Table 1), the distance from the EM source, the operating frequency, and the geometry of the eye. The outermost layers of the eye exhibit the highest electric field intensity. The highest electric field value, 34.95 V/m, is observed at a frequency of 30 GHz. This is attributed to the shorter wavelength of higher frequencies, which are unable to penetrate deeper into the tissues, causing the radiation to be largely absorbed at the surface and resulting in increased absorption in the outer layers.

4.3 SAR distribution

The specific absorption rate (SAR) in the eye is calculated from the electric field distribution using Eq. (3.3). The reported SAR values correspond to the local peak SAR obtained from the numerical simulation. The maximum local SAR values at five 5G frequencies - 2.6, 3.6, 4.4, 18, and

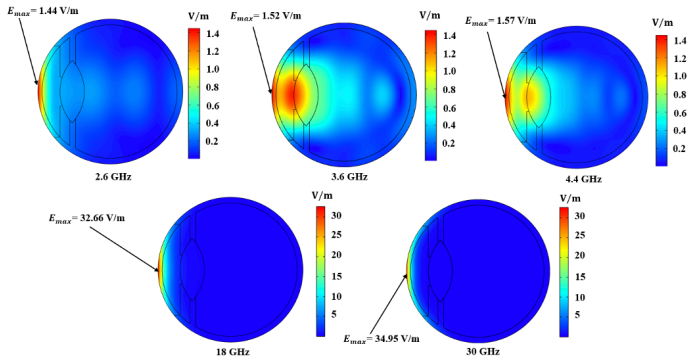


Fig. 7. Electric field distribution in the eye at different 5G frequencies at 0.1 W radiated power.

30 GHz - are 0.018 W/kg, 0.0049 W/kg, 0.0048 W/kg, 11.15 W/kg, and 19.66 W/kg, respectively. Notably, the SAR distribution in the eye does not uniformly follow the electric field distribution across all frequencies. At the lower frequencies (2.6, 3.6, and 4.4 GHz), EM waves have a greater penetration depth, allowing energy to propagate into deeper ocular tissues. Consequently, the maximum SAR occurs in the aqueous humor, whose relatively high electrical conductivity (σ), as shown in Table 1, further enhances EM energy absorption. In contrast, at the higher frequencies (18 and 30 GHz), the penetration depth decreases with increasing frequency, resulting in most of the EM energy being absorbed in the superficial tissues. Consequently, the SAR distribution closely follows the electric field distribution, with the highest SAR values observed in the cornea. This behavior is consistent with the frequency-dependent attenuation of EM waves in biological tissues. Although the calculated local peak SAR values at 18 and 30 GHz are higher than the ICNIRP reference level of 2 W/kg (10 g averaged SAR), direct comparison should be made with caution because the present study reports local peak SAR rather than spatially averaged 10 g SAR. Therefore, the present results should be interpreted as indicators of localized EM energy absorption and thermal behaviour rather than as a regulatory compliance assessment under realistic exposure conditions [4, 8].

4.4 Temperature distribution

The EM energy absorbed by the ocular tissues, as illustrated in Figs. 7-8, is transformed into thermal energy, resulting in a variation of temperature within the different eye layers. The initial and surrounding temperature of the eye model was considered as 37 °C, while tear evaporation effects were neglected in this analysis. The temperature rise in the eye is calculated using Pennes' bio-heat equation (Eq. (3.4)) for an exposure duration of 30 minutes. The maximum temperature values for 2.6, 3.6, 4.4, 18, and 30 GHz are 37.0006°C, 37.0006°C, 37.0005°C, 37.21°C, and 37.237°C, respectively, as shown in Fig. 9. This behavior is influenced by the dielectric characteristics (Table 1) and thermal properties (Table 2) of the ocular tissues, which affect EM energy absorption and heat transfer mechanisms. At 2.6 GHz, the higher electrical conductivity of the aqueous humor leads to a greater temperature rise. The temperature distribution at lower frequencies penetrates deeper into the layers, while

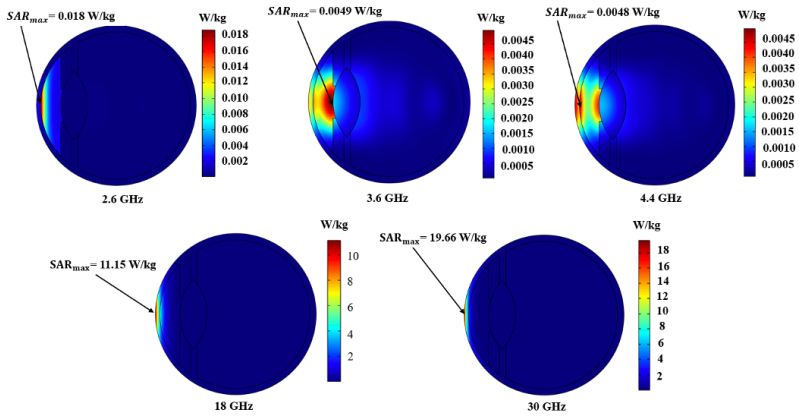


Fig. 8. Specific Absorption Rate (SAR) in the eye at different 5G frequencies at 0.1W radiated power .

at higher frequencies it is mostly in the outer layer. Significant temperature increases of 0.21°C and 0.23°C, are observed at 18 and 30 GHz, respectively. The highest temperature rise among all frequencies occurs at 30 GHz. However, the calculated temperature variations remained within acceptable limits and did not reach levels associated with thermal damage [3, 12]. The relatively small temperature rise obtained in the present study compared with some published studies can be attributed to differences in exposure conditions, radiated power, operating frequency, tissue dielectric properties, and modelling assumptions adopted in numerical simulations. In the present model, tear-film evaporation was neglected, and an insulated thermal boundary condition was applied at the external surface of the eye to simplify the thermal analysis. Future work will incorporate these limitations, to improve the physiological accuracy of the predicted temperature distribution.

4.5 SAR and temperature in the eye at different radiated power

The influence of different input power levels on SAR and temperature variation within the eye tissues was also investigated. Three radiated power 0.05W, 0.1W, and 1W are considered in this study. Fig. 10 presents the maximum SAR and temperature values obtained for each applied power condition. It is found that higher power densities lead to higher value of electric field absorption and therefore higher value of SAR and temperature in the eye. SAR exceeds the limited value for 18 and 30 GHz frequencies at all three power densities. The temperature, however, exceeded the threshold value for 1W radiated power for 18 and 30GHz frequencies.

5. Conclusion

In this research, the effect of 5G radiation on a heterogenous human eye model has been studied. From the results we can conclude that

- SAR has exceeded the threshold value of 2 W/kg for 18 and 30 GHz frequencies.
- The threshold temperature increases of 0.3 °C for the lens and 1°C for the cornea were not exceeded for any of the investigated 5G frequencies.

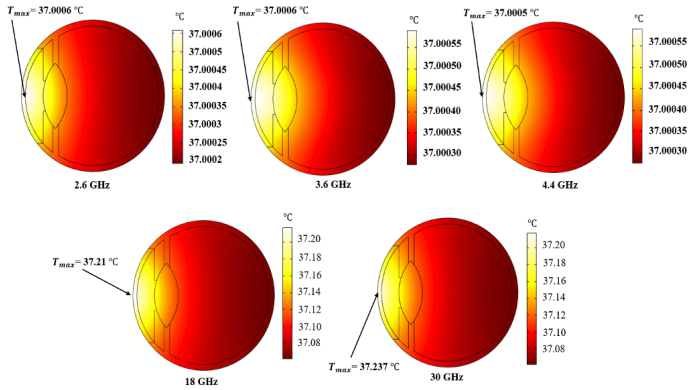


Fig. 9. Temperature distribution in the eye at different 5g frequencies at 0.1 W radiated power for 30 minutes.

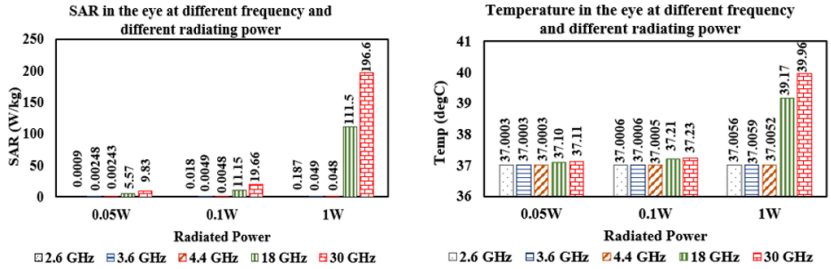


Fig. 10. (a) SAR in the eye at different radiated powers, and (b) temperature in the eye at different radiated powers for 30 min exposure.

Under the simulated exposure conditions, the predicted temperature rise remained below these reported thermal thresholds.

- It was also observed that most of the electric field was absorbed in the outer layer (i.e. cornea layer) of the eye.
- The electric field absorption, SAR, and temperature value seems to decrease as it goes deeper into the tissues. This is because the cornea layer is closer to the radiation source and the dielectric properties of the cornea layer are higher than the rest of the layers.
- Effects of different radiated power on SAR and temperature were also studied and it is observed that at the SAR and temperature in the eye increases as the radiated power increases. The SAR in the eye at 0.1W and 1W exceeded the threshold value, whereas, for temperature the threshold values were exceeded for the 1W power only.
- The present findings are based on a simplified 2D numerical model of the human eye. Therefore, the results should be interpreted within the limitations of the adopted modelling approach and should not be considered a comprehensive assessment of the safety of 5G exposure. Future work

will extend the present study to realistic 3D models, additional exposure scenarios and realistic intermittent exposure duration.

- From a practical perspective, these findings highlight the importance of monitoring both SAR and temperature rise when assessing electromagnetic exposure to ocular tissues, as SAR characterizes electromagnetic energy absorption while temperature rise represents the resulting thermal response.

Acknowledgement

This project is funded by Faculty of Engineering, Kasetsart University (Research Project Code – 67/07/ME), Bangkok, Thailand.

References

[1] Simkó M, Mattsson MO. 5G Wireless Communication and Health Effects-A Pragmatic Review Based on Available Studies Regarding 6 to 100 GHz. Int J Environ Res Public Health. 2019;16(18).

[2] Chiaraviglio L, Elzanaty A, Alouini MS. Health Risks Associated With 5G Exposure: A View From the Communications Engineering Perspective. IEEE Open Journal of the Communications Society. 2021;2:2131-79.

[3] Shafahi M, Vafai K. Human Eye Response to Thermal Disturbances. J Heat Transf. 2010;133(1).

[4] Bhargava D, Rattanadecho P. Numerical Analysis of Specific Absorption Rate and Temperature Distribution in Human Eye due to Moving Electromagnetic Source. Engineered Science. 2023;21:796.

[5] Awada B, Madi G, Mohsen A, Harb A, Diab A, Hamawy L, et al. Simulation of the Effect of 5G Cell Phone Radiation on Human Brain. 2018 IEEE International Multidisciplinary Conference on Engineering Technology (IMCET). 2018:1-6.

[6] Kaburcuk F, Elsherbeni AZ. Efficient Computation of SAR and Temperature Rise Distributions in a Human Head at Wide Range of Frequencies Due to 5 G RF Field Exposure. Applied Computational Electromagnetics Society Journal. 2021;33(11):1236-42.

[7] Aru OE, Adimora KC, Nwankwo FJ. Investigating the impact of 5G radiation on human health using machine learning. Nigerian Journal of Technology. 2021;40(4):694-702.

[8] Aricioglu B, Ferikoglu A. Thermal Effects of 5G Frequency EM Waves on Ocular Tissue. The Applied Computational Electromagnetics Society Journal (ACES). 2021;36(4):286-397.

[9] database IIFtp. [Available from: itis.swiss/virtual-population/tissue-properties/database/dielectric-properties.

[10] Ooi EH, Ng EY. Simulation of aqueous humor hydrodynamics in human eye heat transfer. Comput Biol Med. 2008;38(2):252-62.

[11] Wessapan T, Rattanadecho P. Specific Absorption Rate and Temperature Increase in Human Eye Subjected to Electromagnetic Fields at 900 MHz. J Heat Transf. 2012;134(9):091101-11.

[12] Bernardi P, Cavagnaro M, Pisa S, Piuzzi E. SAR distribution and temperature increase in an anatomical model of the human eye exposed to the field radiated by the user antenna in a wireless LAN. IEEE Trans Microw Theory Tech. 1998;46(12):2074-82.